Neuroradiology Case of the Day

Elliot I. Shoemaker,[1] Allan J. Romano, Mokhtar Gado, and Fred J. Hodges III

Case 1: Chordoma of the Clivus

A 55-year-old woman developed blurred and double vision of the left eye 2 years before these studies. A workup 1 year later showed optic atrophy and a left sixth cranial nerve palsy. Before admission, the patient had two seizures.

Initial noncontrast CT examination showed a low-density mass centered in the left parasellar region, causing bony destruction with a few scattered areas of calcification (Fig. 1A). The contrast examination showed dense homogeneous enhancement of a multilobular mass (Fig. 1B). Definite evidence is present of extension into the left middle cranial fossa and through the incisura of the tentorium into the posterior fossa. On the contrast examination, the floor of the sella appeared intact. An MR examination was obtained with gadolinium. The pre-gadolinium, T1-weighted images showed a low-signal-intensity mass originating from the clivus growing into the suprasellar region with superior and posterior extension (Fig. 1C). The brainstem was deviated posteriorly, and the basal ganglia were displaced superiorly. The postgadolinium, T1-weighted image showed dense homogeneous enhancement (Fig. 1D). The mass showed high signal intensity on the T2-weighted image (Fig. 1E).

Chordoma is a relatively rare neoplasm, accounting for less than 1% of all intracranial tumors [1, 2]. The distribution is approximately 50% sacrococcygeal, 35% cranial, and 15% vertebral [3]. They develop from remnants of the notochord, which is the embryonic precursor of the axial skeleton. This explains their usual midline location. They occur most frequently in the third or fourth decades of life.

These tumors tend to present with the signs and symptoms of a mass compressing the cranial nerves and brainstem, most often the abducens nerve. General symptoms include lethargy, fatigue, and weakness [3].

On CT scans, clival chordomas typically show solitary or multiple areas of low attenuation, probably representing myxoid and gelatinous material found on pathologic examination. Calcification commonly can be seen, representing either tumor calcification or sequestered fragments of bone, and may appear linear, nodular, or mixed. In a review of 30 cases, calcification was present in 47%. The differential diagnosis of a calcified sellar or parasellar lesion would include craniopharyngioma, aneurysm, or meningioma. After contrast injection, clival chordomas are enhanced. The three major directions of tumor growth are parasellar, prepontine, and nasopharyngeal [4].

On T1-weighted MR images, chordomas tend to be isointense or hypointense. T2-weighted images always show high signal intensity. Seventy percent of chordomas show septa of low signal intensity separated by lobulated areas of high signal intensity. Sagittal MR is useful in disclosing the extent of the tumor in the epidural space. Characterization of the tumor is possible with MR imaging [5]. Chordomas are frequently separated into two pathologic subsets described as typical chordomas and chondroid chordomas. The latter tend to have shorter T1 and T2 relaxation times. Overall, chondroid chordomas tend to have a better prognosis than typical chordomas. MR imaging is less accurate than CT in showing calcification and bone destruction.

Elliot I. Shoemaker
Allan J. Romano
Mokhtar Gado

REFERENCES

1. Firooznia H, Pinto RS, Lin JP, Baruch HH, Zausner J. Chordoma: radiologic evaluation of 20 cases. *AJR* **1976**;127:797–805
2. Kendel BE, Lee BC. Cranial chordomas. *Br J Radiol* **1977**;50:687–698
3. Tan WS, Spigos D, Khine N. Chordoma of the sellar region. *J Comput Assist Tomogr* **1982**;6:154–158
4. Meyer JE, Oot RF, Lindfors KK. CT appearance of clival chordomas. *J Comput Assist Tomogr* **1986**;10:34–38
5. Sze G, Uichanco LS, Brant-Zawadzki MN, et al. Chordomas: MR imaging. *Radiology* **1988**;166:187–191

Case 2: Choroid Plexus Papilloma, Third Ventricle

A 3-year-old girl presented with a several-month history of headaches. Physical examination was normal except for increased head circumference. Noncontrast CT scans disclosed hydrocephalus. A mass, isodense with brain parenchyma, partially filled the anterior-superior third ventricle and obstructed CSF outflow at the foramina of Monro (Figs. 2A and

[1] All authors: Mallinckrodt Institute of Radiology, Washington University School of Medicine, 510 S. Kingshighway Blvd., St. Louis, MO 63110. Address reprint requests to M. J. Siegel at this address.

Cases 1 and 4 were prepared by E. I. Shoemaker, A. J. Romano, and M. Gado. Case 2 was prepared by A. J. Romano, E. I. Shoemaker, and M. Gado. Case 3 was prepared by A. J. Romano, E. I. Shoemaker, M. Gado, and F. J. Hodges III. M. J. Siegel is coordinator of the Case of the Day series.

AJR **152:1333–1338, June 1989** 0361–803X/89/1526–1333 © American Roentgen Ray Society

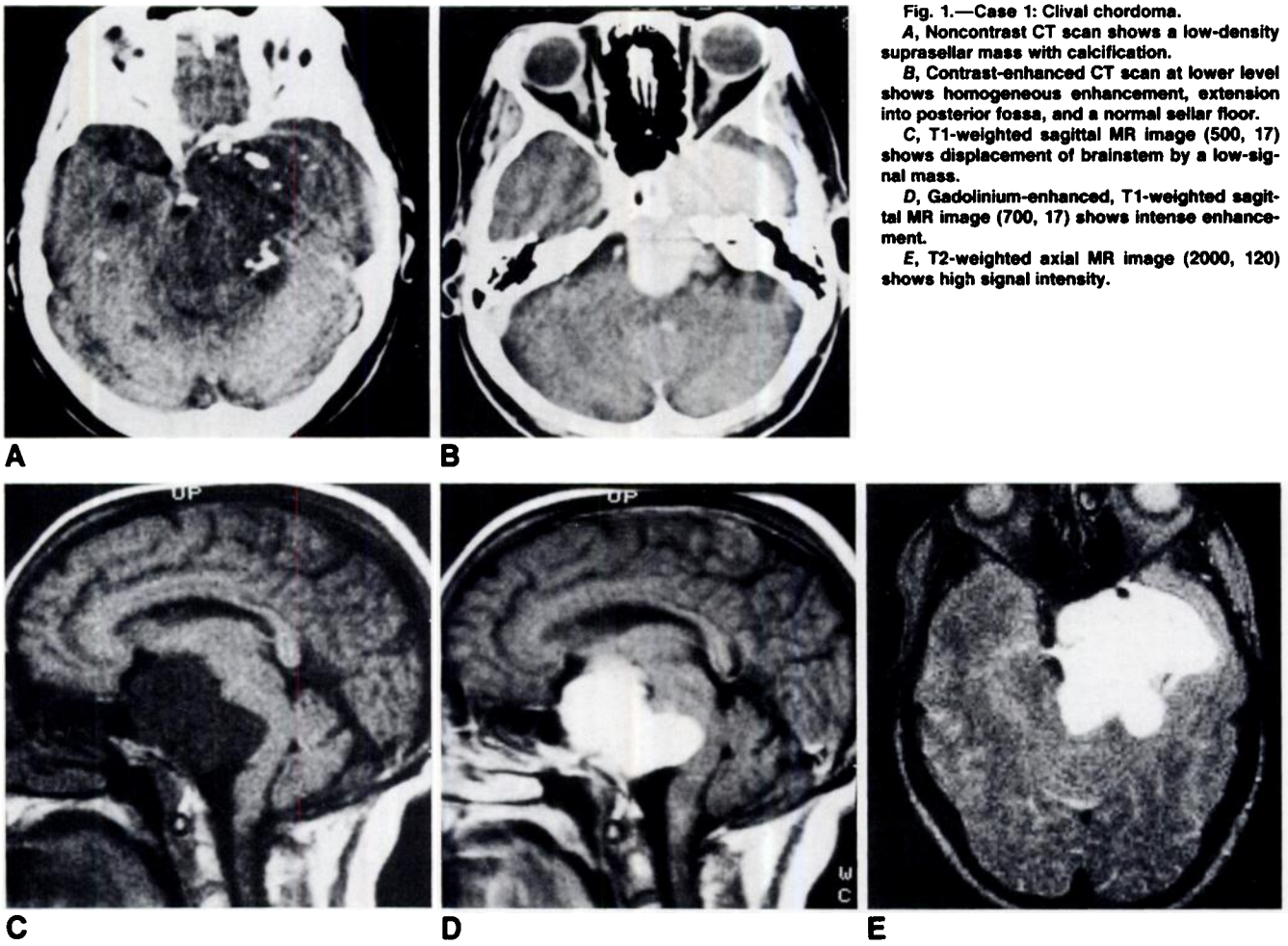

Fig. 1.—Case 1: Clival chordoma.
***A*, Noncontrast CT scan shows a low-density suprasellar mass with calcification.**
***B*, Contrast-enhanced CT scan at lower level shows homogeneous enhancement, extension into posterior fossa, and a normal sellar floor.**
***C*, T1-weighted sagittal MR image (500, 17) shows displacement of brainstem by a low-signal mass.**
***D*, Gadolinium-enhanced, T1-weighted sagittal MR image (700, 17) shows intense enhancement.**
***E*, T2-weighted axial MR image (2000, 120) shows high signal intensity.**

2B). No calcification was shown in the mass. After IV contrast, the mass enhanced intensely and the margins appeared irregular (Fig. 2C). MR images with short and long TR confirmed the location of the mass in the third ventricle and the obstruction at the foramina of Monro (Figs. 2D and 2E). The patient underwent a craniotomy with complete resection of the third ventricle tumor by a transcallosal approach. Histologic examination revealed a benign choroid plexus papilloma.

Choroid plexus papillomas are primary intraventricular neoplasms, accounting for 3% of intracranial neoplasms in children and 0.6% in adults [1, 2]. They arise from the epithelial cells of the choroid plexus and occur wherever choroid plexus is found: lateral ventricles (43%), third ventricle (10%), fourth ventricle (39%), and even the cerebellopontine angles (9%) [2]. In children, papillomas tend to occur in the lateral ventricles, whereas the fourth ventricle is the most common site in adults [1, 3]. In children, 86% of all papillomas occur in the first 5 years of life. Malignant change occurs in up to 20% and is more common in children [3, 4]. Seeding by CSF pathways is reported to occur in both benign and malignant tumors [2, 4]. Choroid plexus papillomas may recur if not completely excised [2, 5].

Patients with choroid plexus papillomas have symptoms of increased intracranial pressure—headaches, vomiting, and gait abnormality. Physical examination shows increased head circumference in children, abnormal plantar reflexes, and papilledema [3, 4]. Hydrocephalus is a constant feature and may be due to obstruction of CSF pathways, overproduction of CSF by the papilloma, adhesions due to bleeding from the tumor, or a combination of these factors [2, 6]. When the tumor is located in the third ventricle, the cause appears to be obstruction of CSF outflow at the foramina of Monro. This is because of the strategic location of third ventricular papillomas, which are attached at the tela choroidea [2, 7]. Sudden death from acute ventricular obstruction is a well-known complication of third ventricular colloid cysts and also has been reported in choroid plexus papillomas of the third ventricle [1].

On CT scans, three fourths of choroid plexus papillomas are isodense or hyperdense relative to brain parenchyma, and one fourth are hypodense or of mixed density. Tumor margins can be smooth (29%), lobulated (19%), or irregular (52%). Irregular margins are found in both malignant tumors (71%) and benign lesions (43%). Calcification is reported in 24%. All choroid plexus papillomas enhance with IV contrast, and the enhancement is typically intense [3].

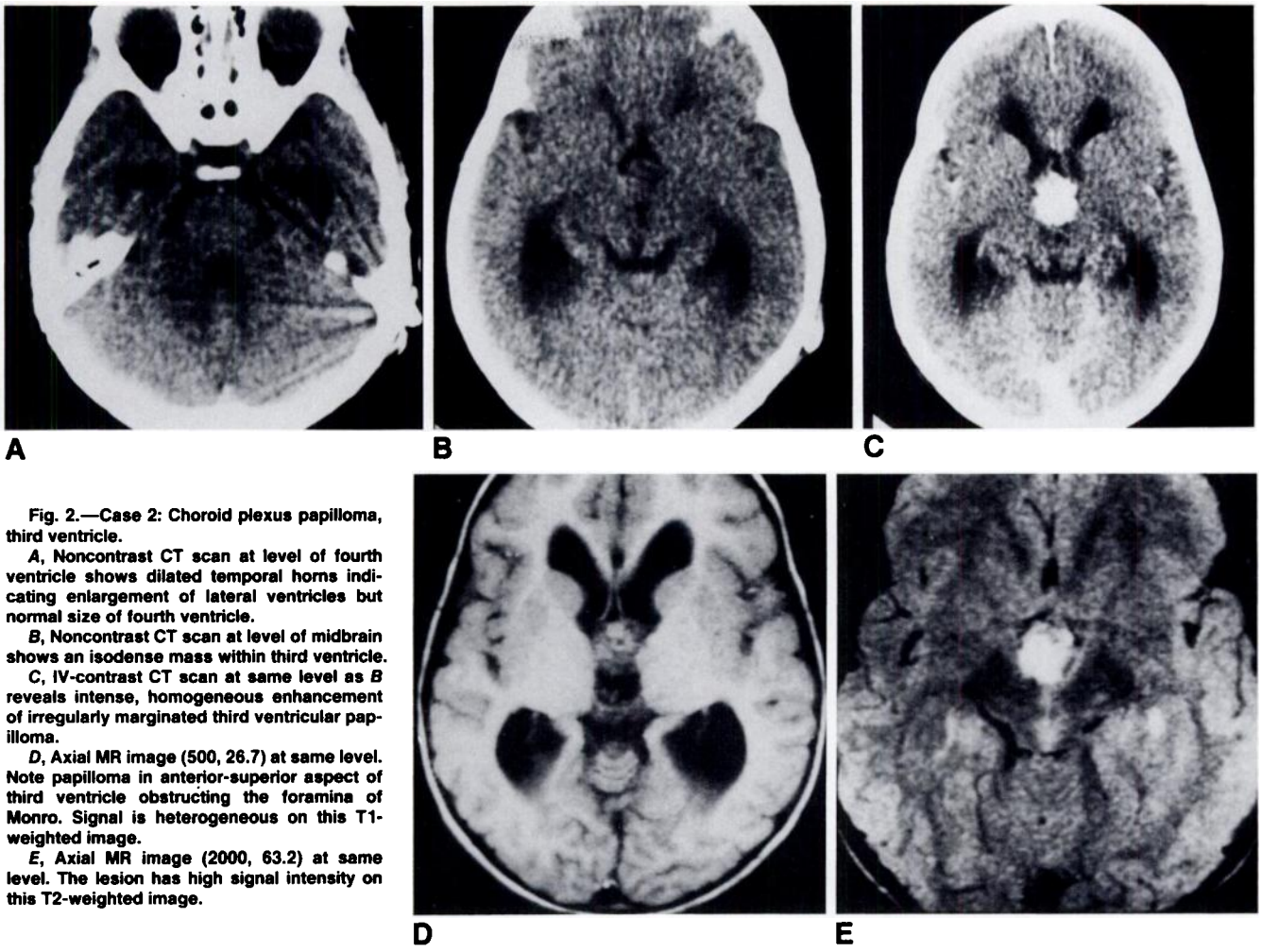

Fig. 2.—Case 2: Choroid plexus papilloma, third ventricle.

***A*, Noncontrast CT scan at level of fourth ventricle shows dilated temporal horns indicating enlargement of lateral ventricles but normal size of fourth ventricle.**

***B*, Noncontrast CT scan at level of midbrain shows an isodense mass within third ventricle.**

***C*, IV-contrast CT scan at same level as *B* reveals intense, homogeneous enhancement of irregularly marginated third ventricular papilloma.**

***D*, Axial MR image (500, 26.7) at same level. Note papilloma in anterior-superior aspect of third ventricle obstructing the foramina of Monro. Signal is heterogeneous on this T1-weighted image.**

***E*, Axial MR image (2000, 63.2) at same level. The lesion has high signal intensity on this T2-weighted image.**

The differential diagnosis of third ventricular tumors includes colloid cyst, meningioma, craniopharyngioma, glioma, ependymoma, dermoid, epidermoid, metastasis, and tumors deposited by CSF seeding. CT and MR features can be used to exclude colloid cyst, meningioma, most craniopharyngiomas, dermoid, and epidermoid tumors [3, 4, 7]. In a young patient, metastasis is unlikely. Supratentorial ependymomas tend to have a smaller intraventricular component compared with a larger portion of the tumor mass invading the adjacent parenchyma. In a child, the most common tumor to spread via CSF pathways is medulloblastoma, but this characteristically involves the cerebellar vermis initially [7]. The features possessed by gliomas and choroid plexus papillomas overlap considerably, making reliable distinction between these tumor types difficult [3].

Allan J. Romano
Elliot I. Shoemaker
Mokhtar Gado

REFERENCES

1. Gradin WC, Taylor C, Fruin AH. Choroid plexus papilloma of the third ventricle: case report and review of the literature. *Neurosurgery* **1983**;12:217–220
2. Rovit RL, Schechter MM, Chodraff P. Choroid plexus papillomas—observations on radiographic diagnosis. *AJR* **1970**;110:608–617
3. Kendall B, Reider-Grosswasser I, Valentine A. Diagnosis of masses presenting within the ventricles on computed tomography. *Neuroradiology* **1983**;25:11–22
4. Thompson JR, Harwood-Nash DC, Fitz CR. The neuroradiology of childhood choroid plexus neoplasms. *AJR* **1973**;118:116–132
5. Tomasello F, Albanese V, Bernini FP, Picozzi P. Choroid plexus papilloma of the third ventricle. *Surg Neurol* **1981**;16:69–71
6. Jooma R, Grand DN. Third ventricle choroid plexus papillomas. *Childs Brain* **1983**;10:242–250
7. Hopper KD, Foley C, Nieves NL, Smirniotopoulos JG. The interventricular extension of choroid plexus papillomas. *AJNR* **1987**;8:469–472

Case 3: Plasmacytoma of the Skull Vault

A 70-year-old man presented with a 6-month history of progressive decline in cognitive function, lethargy, and mild ataxia. Laboratory evaluation disclosed anemia, hyperproteinemia, increased erythrocyte sedimentation rate, and elevated 24-hour urine protein level. Serum and urine electrophoresis was positive for IgG kappa paraprotein and kappa light chains. Noncontrast CT showed a large hyperdense mass with focal calcifications. The lesion crossed the midline without displacing the adjacent falx cerebri (Fig. 3A). Bone

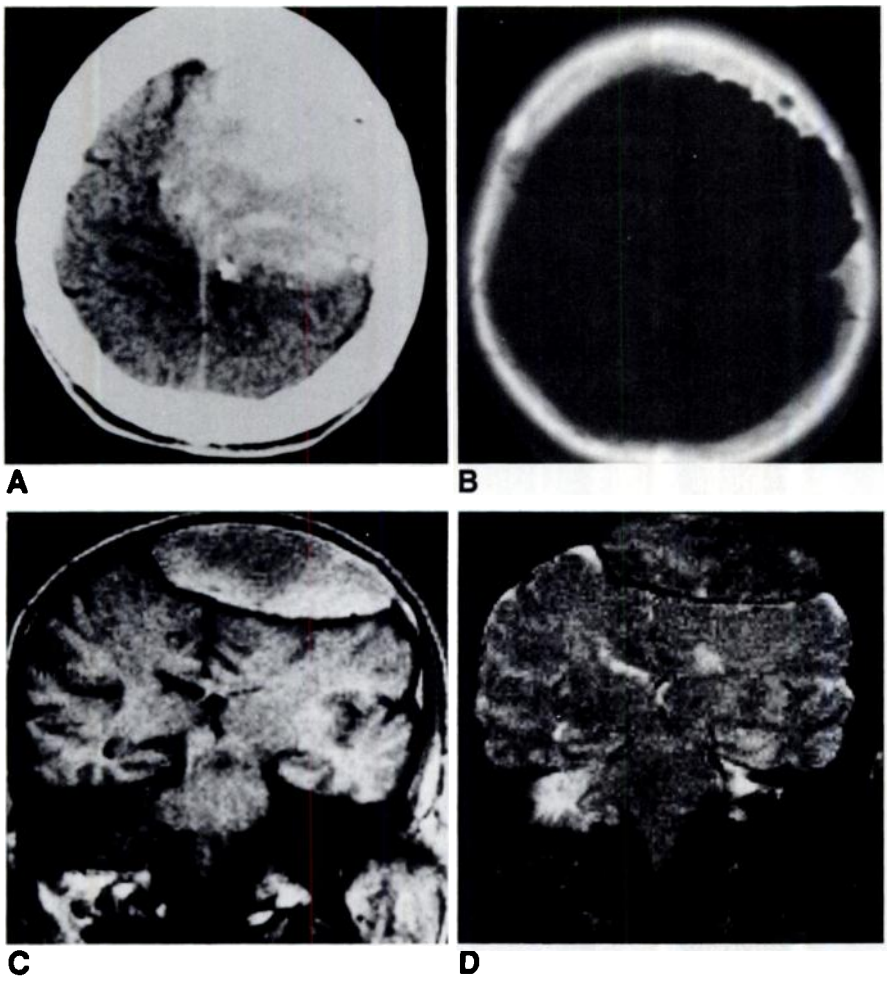

Fig. 3.—Case 3: Plasmacytoma of skull vault.
***A*, Noncontrast axial head CT scan near vertex shows a hyperdense mass, with focal areas of higher density suggesting calcification. Lesion crosses midline.**
***B*, Bone windows of scan *A*, showing scalloping of inner table of skull, penetrating diploic space.**
***C*, Coronal MR image (700, 17). Elliptical extradural mass crosses midline and involves inner table and diploic space. It has mixed signal intensity, but generally has a slightly higher signal than brain parenchyma.**
***D*, Coronal MR image (2000, 120). Heterogeneous signal is again noted on this long sequence image. Black line along inner margin of mass represents dura, confirming extradural location.**

windows showed erosion of the inner table of the skull extending into the diploic space with preservation of the outer table of bone (Fig. 3B). Coronal short- and long-sequence MR images identified the mass as extradural, with inward displacement of the intact dura and distortion of the adjacent brain and lateral ventricles. Although the cerebral hemispheres were distorted, there was no signal abnormality in the brain (Figs. 3C and 3D). A skeletal survey revealed no definite evidence for other bone lesions. Bone-marrow biopsy showed a mildly cellular marrow with 70–80% plasma cells, consistent with multiple myeloma. A stereotaxic biopsy of the skull lesion confirmed the diagnosis of plasma cell myeloma.

Multiple myeloma accounts for 1% of all malignant disease and slightly greater than 10% of hematologic malignancies [1]. This neoplasm originates from plasma cells, which are derived from the B-lymphocyte [2]. Myeloma is characterized by proliferation of a single clone of abnormal plasma cells, which produce abnormal monoclonal proteins [1]. Three forms of plasma cell proliferation are recognized—solitary plasmacytoma of bone, extramedullary plasmacytoma, and multiple myeloma. These are felt to be different manifestations of the same disease [3, 4]. The criteria for the diagnosis of multiple myeloma are (1) increased numbers of abnormal, atypical, or immature plasma cells in the bone marrow, and (2) monoclonal protein in the serum or urine, or (3) bone lesions consistent with myeloma [1].

The disease generally occurs in patients between 50 and 70 years old, is more common in men (61%), is typically associated with abnormal protein in both serum (90%) and urine (80%), and presents most often with bone pain (68%). At presentation, 79% of patients have abnormal skeletal radiographs [1]. The flat bones containing red marrow (ribs, vertebrae, sternum, skull, pelvis, and mandible) are involved most often [5].

Although the radiographic presentation is variable, focal abnormalities typically appear as multiple small, rather uniform osteolytic lesions with sharp punched-out margins [1, 2, 5, 6, 7]. This is certainly the classic appearance in the skull, where the earliest lesions may be most conspicuous. Small lesions may coalesce into larger areas of bone destruction. Rarely, a large solitary lesion is observed. The involvement of bone is often associated with an adjacent soft-tissue mass [8]. In the skull, unusually large solitary lesions with an associated soft-tissue mass have rarely been reported to cause deformity of the brain and can be associated with neurologic symptoms due to cerebral compression [9].

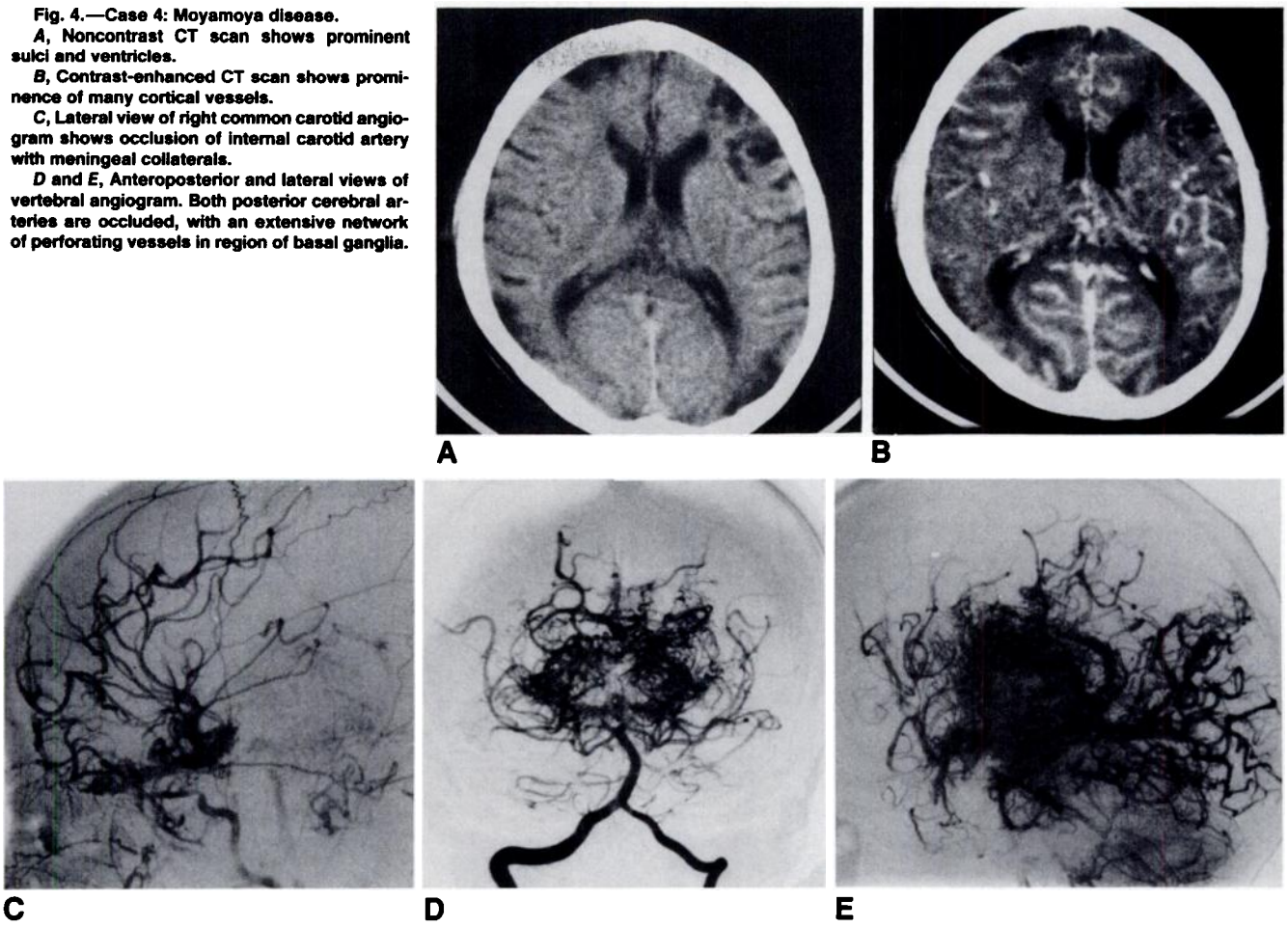

Fig. 4.—Case 4: Moyamoya disease.
***A*, Noncontrast CT scan shows prominent sulci and ventricles.**
***B*, Contrast-enhanced CT scan shows prominence of many cortical vessels.**
***C*, Lateral view of right common carotid angiogram shows occlusion of internal carotid artery with meningeal collaterals.**
***D* and *E*, Anteroposterior and lateral views of vertebral angiogram. Both posterior cerebral arteries are occluded, with an extensive network of perforating vessels in region of basal ganglia.**

The differential diagnosis includes metastasis, osteochondroma, osteochondrosarcoma, meningioma, sarcoma of the dura, and hemangioma of the dura. The sharp borders, little or no bony sclerosis or new bone formation, and the paucity of periosteal reaction are useful in suggesting the correct diagnosis of plasmacytoma. However, in cases of unusual presentation, such as a solitary expansile lesion of considerable size, or advanced disease, reliable distinction may be impossible.

Allan J. Romano
Elliot I. Shoemaker
Mokhtar Gado
Fred J. Hodges, III

REFERENCES

1. Kyle RA. Multiple myeloma, review of 869 cases. *Mayo Clin Proc* **1975**;50:29–40
2. Goodman MA. Plasma cell tumors. *Clin Orthop* **1986**;204:86–92
3. Tong D, Griffin TW, Laramore GE, et al. Solitary plasmacytoma of bone and soft tissues. *Radiology* **1980**;135:195–198
4. Meyer JE, Schulz MD. "Solitary" myeloma of bone. A review of 12 cases. *Cancer* **1974**;34:438–440
5. Edeiken J, Hodes PJ. *Roentgen diagnosis of diseases of bone*, 2nd ed. Baltimore: Williams & Wilkins, **1973**:1026–1051
6. Meszaros WT. The many facets of multiple myeloma. *Semin Roentgenol* **1974**;9:219–228
7. Yentis I. Radiological aspects of myelomatosis. *Clin Radiol* **1961**;12:1–7
8. Resnick D, Niwayama G. *Diagnosis of bone and joint disorders*, 2nd ed. Philadelphia: Saunders, **1988**:2360–2379
9. Stork RJ, Henson RA. Cerebral compression by myeloma. *J Neurol Neurosurg Psychiatry* **1981**;44:833–836

Case 4: Moyamoya Disease

The patient is a 10½-year-old boy with Down syndrome. An episode of lethargy, fever, and right-sided weakness of several weeks duration occurred approximately 2 years before admission. During the few months before this study, the parents noted progressive intermittent right-sided weakness, particularly when the patient exercised.

The noncontrast CT examination showed prominent sulci and ventricles but no parenchymal changes (Fig. 4A). The contrast study showed intense enhancement of many cortical vessels bilaterally (Fig. 4B). An angiogram was obtained. Contrast-material injection in the right common carotid artery showed occlusion of the internal carotid artery just distal to the takeoff of the ophthalmic artery. Enlarged meningeal branches perforated the dura and supplied the anterior portion

of the middle cerebral artery as well as callosomarginal branches anteriorly (Fig. 4C). The contrast-material injection in the left internal carotid artery showed similar findings. Selective injection in the right vertebral artery showed occlusion of the posterior cerebral arteries at their origins. An extensive network of perforating vessels, supplied via the basilar artery, appeared to reconstitute branches of the posterior cerebral artery as well as posterior branches of the middle cerebral artery. These perforating vessels were most prominent in the region of the basal ganglia (Figs. 4D and 4E). The overall appearance was consistent with Moyamoya disease.

In general, Moyamoya disease causes occlusion or stenosis of the supraclinoid portions of the internal carotid arteries, as well as the proximal portions of the anterior and middle cerebral arteries. It tends to be bilateral. The most striking source of collaterals is the dense network of small conglomerate vessels in the region of the basal ganglia and upper brainstem. The anterior or middle cerebral arteries beyond the site of occlusion may be reconstituted by way of this network. Vessels that contribute to this network include the thalamoperforate arteries, the anterior choroidal arteries, and the artery of Heubner, to name a few. Transdural external-to-internal carotid anastamoses can occur via the superficial temporal artery, middle meningeal artery, occipital artery, or the ophthalamic artery. These are called meningeal anastomoses. End-to-end anastamoses on the surface of the cerebral hemispheres can occur, unless the basilar artery is occluded, and are called leptomeningeal anastamoses [1, 2].

Typically, most of these patients are less than 15 years old. Young patients can present with sudden and recurrent paresis of one or two limbs, as well as convulsive seizures. Overall, symptoms due to cerebral ischemia are the main features in childhood. In adults, subarachnoid hemorrhage is the most common presentation [3]. These patients present with motor weakness, decreased sensation, mental deterioration, and convulsions or headache. In a large series of 96 cases, 10 of the patients had symptoms before the age of 10 years and 73 had symptoms before 24 years of age [1].

In a CT study of 12 patients with Moyamoya disease, moderate dilatation of the ventricular system was found in seven, widening of the sulci in nine, and intracerebral lucent foci representing old infarcts in 11 patients. Most of these features were in the cortex or subcortical white matter [4]. In another study of six patients, focal low-density areas were found in five patients and were felt to represent previous infarcts. The postcontrast CT scans showed curvilinear tortuous densities in the basal ganglia in four patients. Vessels in the cerebral sulci and sylvian fissures were often not seen except in those patients in whom angiography showed extensive parenchymal and leptomeningeal collaterals [3].

Elliot I. Shoemaker
Allan J. Romano
Mokhtar Gado

REFERENCES

1. Taveras JM. Multiple progressive intracranial arterial occlusion: a syndrome of children and young adults. *AJR* **1969**;106:235–268
2. Handa J, Handa H. Progressive cerebral arterial occlusive disease: analysis of 27 cases. *Neuroradiology* **1972**;3:119–133
3. Takahashi M, Miyauchi T, Kowada M. Computed tomography of Moyamoya disease: demonstration of occluded arteries and collateral vessels as important diagnostic signs. *Radiology* **1980**;134:671–676
4. Handa J, Nakano Y, Dkuno T, Komuro H, Hojyo H, Handa H. Computerized tomography in Moyamoya syndrome. *Surg Neurol* **1977**;7:315–319